



**Rapid Isolation of Extracellular Vesicles from Diverse Biofluid Matrices via Capillary-Channeled Polymer Fiber Solid-Phase Extraction Micropipette Tips**

Journal:	<i>Analyst</i>
Manuscript ID	AN-ART-03-2021-000373.R1
Article Type:	Paper
Date Submitted by the Author:	10-May-2021
Complete List of Authors:	Jackson, Kaylan; Clemson University, Department of Chemistry Powell, Rhonda; Clemson University, Light Imaging Facility Bruce, Terri; Clemson University, Department of Bioengineering Marcus, R.; Clemson University, Department of Chemistry

1  
2  
3  
4  
5  
6  
7  
8  
9  
10  
11  
12  
13  
14  
15  
16  
17  
18  
19  
20  
21  
22  
23  
24  
25  
26  
27  
28  
29  
30  
31  
32  
33  
34  
35  
36  
37  
38  
39  
40  
41  
42  
43  
44  
45  
46  
47  
48  
49  
50  
51  
52  
53  
54  
55  
56  
57  
58  
59  
60

**Rapid Isolation of Extracellular Vesicles from Diverse Biofluid  
Matrices via Capillary-Channeled Polymer Fiber Solid-Phase  
Extraction Micropipette Tips**

Kaylan K. Jackson<sup>1</sup>, Rhonda R. Powell<sup>2</sup>, Terri F. Bruce<sup>3</sup>, R. Kenneth Marcus<sup>1\*</sup>

<sup>1</sup>Clemson University, Department of Chemistry, Clemson, SC 29634

<sup>2</sup>Clemson University, Clemson Light Imaging Facility, Clemson, SC 29634

<sup>3</sup>Clemson University, Department of Bioengineering, Clemson, SC 29634

\* Author to whom correspondence should be addressed

Submitted as a Research Article in Analyst

## Abstract

Extracellular vesicles (EVs) play essential roles in biological systems based on their ability to carry genetic and protein cargos, intercede in cellular communication and serve as vectors in intercellular transport. As such, EVs are species of increasing focus from the points of view of fundamental biochemistry, clinical diagnostics, and therapeutics delivery. Of particular interest are 30 – 200 nm EVs called exosomes, which have demonstrated high potential for use in diagnostic and targeted delivery applications. The ability to collect exosomes from patient biofluid samples would allow for comprehensive yet remote diagnoses to be performed. While several exosome isolation methods are in common use, they generally produce low recoveries, whose purities are compromised by concomitant inclusion of lipoproteins, host cell proteins, and protein aggregates. Those methods often work on lengthy timescales (multiple hours) and result in very low throughput. In this study, capillary-channeled polymer (C-CP) fiber micropipette tips were employed in a hydrophobic interaction chromatography (HIC) solid-phase extraction (SPE) workflow. Demonstrated is the isolation of exosomes from human urine, saliva, cervical mucus, serum, and goat milk matrices. This method allows for quick (< 15 min) and low-cost (< \$1 per tip) isolations at sample volume and time scales relevant for clinical applications. The tip isolation was evaluated using absorbance (scattering) detection, nanoparticle tracking analysis (NTA), and transmission electron microscopy (TEM). Exosome purity was assessed by Bradford assay, based on the removal of free proteins. An enzyme-linked immunosorbent assay (ELISA) to the CD81 tetraspanin protein was used to confirm the presence of the known exosomal-biomarker on the vesicles.

**Keywords:**

Extracellular vesicles (EVs), Exosomes, Capillary-channeled polymer (C-CP), Solid-phase extraction (SPE), Hydrophobic interaction chromatography (HIC)

**Introduction**

Extracellular vesicles (EVs) are a diverse group of cell-derived membrane vesicles, typically ranging in size from 30 nm to 1  $\mu\text{m}$  in diameter.<sup>1, 2</sup> EVs are released by all cell types and contain the biomolecular characteristics of the mother cell (i.e., DNA, RNA, miRNA, mRNA, biomarker proteins).<sup>3-7</sup> While no official EV classification system exists, three main EV subtypes have been identified based on size and mechanism of biogenesis.<sup>8, 9</sup> Microvesicles are 100 nm to 1  $\mu\text{m}$  vesicles created by the outward budding of a cell membrane. Apoptotic bodies (reflective of cell death<sup>10</sup>) are 1 to 5  $\mu\text{m}$  vesicles created during the programmed cell death process. Exosomes are 30 to 200 nm vesicles created through the multivesicular body (MVB) endosomal pathway. Due to their similarities in composition, overlapping size range, and characteristic cup/dimpled shape when observed by electron microscopy, the exosome and microvesicle subtypes are difficult to differentiate. For this reason, the vesicles are generically referred to as EVs.<sup>11</sup> Not surprisingly, within the heterogeneity in EV sources, size, and content, the specific mechanisms of action and distribution of potential biomarkers varies immensely.<sup>12</sup>

EVs are primary vehicles in intercellular communication, signal transduction, and local and distal transport processes.<sup>13, 14</sup> The exosome subset of EVs has become

1  
2  
3 increasingly targeted both as mediums for diagnostic information and cargo  
4  
5 transmission.<sup>15, 16</sup> The lack of understanding of EV physiochemical and biological  
6  
7 characteristics, along with a lack of field-wide consensus, has hindered the progress of  
8  
9 the fundamental and clinical use of exosomes. A thorough understanding of exosome  
10  
11 biophysical attributes would allow for details of several vital cell interaction mechanisms  
12  
13 to be revealed (i.e., immune regulation, communication, and disease progression).<sup>17, 18</sup>  
14  
15 The analysis of EV-associated biomarker components during liquid biopsies has  
16  
17 become a valued tool for cancer detection, allowing for the surveillance of progression  
18  
19 and treatment with a reduced physical burden on the patient.<sup>16, 19</sup> Alternatively, the  
20  
21 large-scale processing of exosomes has become a key goal for researchers in many  
22  
23 areas, including in the biopharmaceutical industry. EVs from mesenchymal stem cell  
24  
25 (MSC) origin are of particular interest, having demonstrated the ability to enhance  
26  
27 therapeutic transport of targeted drugs,<sup>20</sup> initiate tissue regeneration,<sup>21</sup> and support  
28  
29 immune response modulation.<sup>14</sup> Nevertheless, for the full extent of EV analyses to be  
30  
31 realized, the inefficient tools for EV retrieval must be addressed.  
32  
33  
34  
35  
36

37  
38 Due to their ubiquitous nature in terms of the cells of origin, exosomes and other  
39  
40 EVs are found in diverse biofluids, including urine,<sup>22-24</sup> saliva,<sup>25-27</sup> blood (serum and  
41  
42 plasma)<sup>28-30</sup>, cervical mucus<sup>25, 31, 32</sup>, breast milk<sup>20-22</sup>, and cerebrospinal,<sup>33, 34</sup> lymph,<sup>35, 36</sup>  
43  
44 synovial,<sup>37</sup> and amniotic<sup>38</sup> fluids. As such, these media are reservoirs to derive clinical  
45  
46 and research scale populations. EVs may also be harvested from cell culture media  
47  
48 during the cell growth process for fundamental studies or subsequent use as  
49  
50 biotherapeutic vectors.<sup>39</sup> Despite the high bioavailability of EVs, the extraction of EVs  
51  
52 from biofluids has proven to be a challenge due to sample and vesicle heterogeneity  
53  
54  
55  
56  
57  
58  
59  
60

1  
2  
3 and intense matrix effects. In terms of characterizing the effectiveness of generic EV  
4 isolation processes, several metrics exist relative to the final product's quality (versus  
5 the cost/time aspects of the procedures). The first, most obvious feature is the yield;  
6 how many microvesicles can be extracted per unit volume of the primary matrix.  
7  
8 Practical working volumes can range from tens of microliters of cerebrospinal fluid  
9 (CSF) to milliliters of urine and liters of cell culture media. The second is the purity of  
10 the isolate. In the case of EVs, the primary contaminants/co-eluates are matrix and  
11 host cell proteins. In the case of serum/plasma samples, these would typically include  
12 albumins and, most problematically, lipoproteins.<sup>40, 41</sup> Finally, the most critical aspect is  
13 the retention of biological functionality. Whether the end-use is clinical analysis,  
14 fundamental research, or production of biotherapeutic vectors, the recovered EVs'  
15 physical and chemical integrity must remain intact. Additional metrics come into play  
16 during high-specificity isolations of targeted EV populations. In all instances, aspects  
17 regarding processing time, capital and supply costs, and operational complexity must be  
18 considered.

19  
20  
21 It has been documented the needs for the development and optimization of  
22 methods specifically for the isolation and quantification of EVs from complex biofluid  
23 samples.<sup>42</sup> The available methods for these purposes limit the downstream  
24 characterization and application of EV recoveries due to concentration and purity  
25 concerns. The lack of efficient EV isolation methods has become the rate-limiting step  
26 towards realizing the full potential of EVs in clinical and fundamental research and  
27 prevents large-scale processing of EVs. Many EV isolation methods are available based  
28 on a wide variety of chemical/physical properties. Riekkola and co-workers have  
29  
30  
31  
32  
33  
34  
35  
36  
37  
38  
39  
40  
41  
42  
43  
44  
45  
46  
47  
48  
49  
50  
51  
52  
53  
54  
55  
56  
57  
58  
59  
60

1  
2  
3 recently presented an excellent review of the topic,<sup>43</sup> with many papers describing  
4 comparisons of the methods. At this point, it is clear that no single method can be  
5  
6 universally applied.<sup>44, 45</sup> The employed isolation method is usually chosen based on  
7  
8 the subsequent means of characterization and utilization of the EVs. At present,  
9  
10 ultracentrifugation (UC) methods are most commonly used to isolate EVs.<sup>46</sup> The UC  
11  
12 isolation method consists of several differential centrifugation steps, potentially reaching  
13  
14 200,000  $\times g$ .<sup>13</sup> UC introduces high-costs regarding time (2 hours to overnight), sample  
15  
16 volume (10 - 45 mL), and capital (up to \$100,000 for equipment, and \$3,000 in running  
17  
18 costs per year), producing low recovery/yields (5-25%) which are typically contaminated  
19  
20 with protein/lipoprotein aggregates.<sup>46, 47</sup> Variations of this technique employing density  
21  
22 gradients and other reagents have also been implemented but continue to present the  
23  
24 previously-mentioned challenges.<sup>46, 48</sup> Other size/density-based methods include  
25  
26 ultrafiltration, size-exclusion spin downs, and field flow fractional.<sup>49-51</sup> Here again, low  
27  
28 purity recoveries are problematic. As a final class of methods, immune-affinity and  
29  
30 polymer precipitation “kits” are finding increased use.<sup>52, 53</sup> Still, concerns lie in the low  
31  
32 yield and impure recoveries, skewing the downstream characterization of the vesicles.  
33  
34 Ultimately, an isolation method with the ability to efficiently produce high-yield, high-  
35  
36 purity EVs on practical time/cost scales is of critical importance.  
37  
38  
39  
40  
41  
42  
43

44 To address the aforementioned issues, researchers from the Bruce and Marcus  
45  
46 groups have demonstrated the use of a polyester (PET) capillary-channeled polymer  
47  
48 (C-CP) fiber stationary phase in hydrophobic interaction chromatography (HIC)  
49  
50 workflows for EV isolation.<sup>54-60</sup> The C-CP fibers consist of an 8-legged periphery that  
51  
52 creates 1 to 4  $\mu\text{m}$ -wide channels upon colinear packing in a column format. The relative  
53  
54  
55  
56  
57  
58  
59  
60

1  
2  
3 hydrophobicity of the stationary phase and the high-salt retention of the EVs allows for  
4  
5 the capture and elution of the vesicles based on hydrophobicity. HIC has been  
6  
7 traditionally applied to protein separations<sup>61</sup> due to the non-denaturing, on-off  
8  
9 partitioning of the solute, allowing the preservation of structure/function.<sup>62-64</sup> Taking  
10  
11 advantage of this, the efficient and vesicle-preserving isolation of EVs from urine,<sup>54, 56</sup>  
12  
13 blood plasma,<sup>55</sup> and cell culture milieu<sup>54, 58</sup> have been demonstrated in a 10-min HPLC  
14  
15 workflow enabling simultaneous EV isolation and quantification. Importantly, recent  
16  
17 proteomics analysis of the eluates has revealed a very efficient removal of serum  
18  
19 proteins and lipoproteins, yielding extremely high purity fractions in comparison to other  
20  
21 methods.<sup>59</sup> The method has been extended to a more clinically-favorable EV isolation  
22  
23 workflow using 1-cm C-CP fiber phases attached to micropipette tips, allowing for the  
24  
25 solid-phase extraction (SPE) of EVs to occur in a table-top centrifuge.<sup>57</sup> Both methods  
26  
27 have proven to be beneficial in terms of efficiency, purity, and yield, producing  
28  
29 recoveries of EVs on clinically relevant scales of time (< 15 minutes) and cost (< \$1 per  
30  
31 column/tip). Here, the versatility of the C-CP fiber spin-down tip to produce  
32  
33 concentrated and contaminant-free EV recoveries is demonstrated for the complex  
34  
35 matrices of urine, saliva, cervical mucus, serum, and milk. The tip recovery of  
36  
37 exosomes was evaluated using absorbance (scattering) detection, nanoparticle tracking  
38  
39 analysis (NTA), and transmission electron microscopy (TEM). The exosome purity was  
40  
41 assessed by Bradford assay of free proteins. The bioactivity and identity of the  
42  
43 recovered vesicles was confirmed with an enzyme-linked immunosorbent assay  
44  
45 (ELISA) to the CD81 tetraspanin protein. It is believed that the methodology presented  
46  
47 here will have relevance to both clinical and fundamental biology research settings.  
48  
49  
50  
51  
52  
53  
54  
55  
56  
57  
58  
59  
60



## Experimental

*Chemicals and reagents* - Deionized water (DI-H<sub>2</sub>O, 18.2 MΩ-cm) was obtained from a Milli-Q water purification system (Millipore Sigma, Merck, Darmstadt, Germany).

Biotechnology-grade glycerol and ammonium sulfate were purchased from VWR (Sokom, OH, USA). Phosphate buffered saline (PBS, pH = 7.4), bovine serum albumin (BSA), and Pierce™ Coomassie Plus (Bradford) Assay Reagent were purchased from ThermoFisher Scientific (Waltham, MA, USA).

*Instrumentation* - A NanoVue Plus UV-Vis spectrophotometer (GE Healthcare, Chicago, IL, USA) was used to measure the absorbance/scattering (203 nm) of the EV fractions. A Synergy H1 Hybrid Multi-Mode Plate Reader (BioTek, Winooski, VT, USA) was used to measure the UV-Vis absorbance (595 nm) of samples in the 96 cell-well format during the Bradford assay of protein content, employing the colorimetric Pierce™ Coomassie Plus (Bradford) Assay Reagent. The plate reader was also used in the chemiluminescent detection of the Pierce™ ECL Substrate during the enzyme-linked immunosorbent (ELISA) assay. A Hitachi HT7830 transmission electron microscope (Chiyoda City, Tokyo, Japan) was used for TEM imaging to determine the structural integrity, size, and purity of the EVs in the C-CP tip recoveries from various biofluids. A Malvern Panalytical NanoSight NS300 nanoparticle tracking analysis (NTA) system (Malvern, Worcestershire, United Kingdom) was used to determine the concentration and size distribution of isolated vesicles.

*Extracellular vesicles* - Commercial lyophilized “exosome standards” from the urine of healthy donors were obtained from Galen Laboratories Supplies (Craigavon, Northern Ireland). To be clear, the material has not been certified as a reference standard. No

1  
2  
3 information regarding purity or classification was supplied from the manufacturer.  
4  
5 However, the product is a means of preparing EV solutions of known concentration (2.7  
6  
7  $\times 10^{12}$  particles  $\text{mL}^{-1}$ ), though vesicles exceeding typical exosome diameter,  
8  
9 lipoproteins, and other protein contaminants have been previously identified in the  
10  
11 material.<sup>65</sup> Despite the potential of systematic error (impurities) introduced by these  
12  
13 standards, they have proven useful for order-of-magnitude estimation of recovered EV  
14  
15 concentrations.  
16  
17

18  
19 Fresh-morning urine, saliva, and cervical mucus (collected using a cotton swab  
20  
21 and dissolved in PBS) were obtained from consenting, anonymous donors. After sample  
22  
23 collection, the cervical mucus samples were stored at  $-80^{\circ}\text{C}$  until thawed for EV  
24  
25 processing. Corning™ Human AB Blood Serum was obtained from ThermoFisher  
26  
27 Scientific (Waltham, MA, USA). The frozen human serum was thawed and aliquoted  
28  
29 before use. Unpasteurized raw goat milk (serving as a surrogate for human breast milk)  
30  
31 was obtained from Split Creek Farm (Anderson, SC, USA). All biofluid samples were  
32  
33 filtered using a sterile syringe filter of  $0.22\ \mu\text{m}$  pore size (Frogga Bio, Toronto, Canada)  
34  
35 prior to processing.  
36  
37

38  
39  
40 *C-CP Fiber Tip Creation and Methodology* - The C-CP fiber micropipette tips were  
41  
42 assembled as previously reported,<sup>57</sup> with the same HIC isolation workflow employed.  
43  
44 Briefly, the 1-cm long C-CP fiber tips were cut from 30-cm long, 0.8 mm inner diameter  
45  
46 fluorinated ethylene-propylene (FEP) C-CP packed columns consisting of ~450 PET C-  
47  
48 CP fibers. The C-CP tips had an interstitial fraction of ~0.6, with ~3  $\mu\text{L}$  of bed volume,  
49  
50 which was press-fit to 200  $\mu\text{L}$  low-retention micropipette tips and secured with a small  
51  
52 amount of superglue, as depicted in Fig. 1. The EV isolation methodology for the  
53  
54  
55  
56  
57  
58  
59  
60

1  
2  
3 various biofluids was initiated by mixing 100  $\mu\text{L}$  of the raw biofluid with 100  $\mu\text{L}$  of  
4 ammonium sulfate (2M final concentration) to induce the hydrophobic interaction  
5 between the biofluid components and the fibers. The total volume was vortexed, then  
6 deposited inside the sample reservoir of the C-CP tip assembly. The apparatus was  
7 then placed inside a 15-mL conical, table-top centrifuge tube and spun-down at 300 x g  
8 for 1 minute. (Due to the high viscosity of the saliva matrix, the tip containing the saliva  
9 sample was centrifuged at 500 x g for 10 minutes.) Next, the fiber-bound vesicles were  
10 washed with 200  $\mu\text{L}$  of DI-water (300 x g, 1 min.) before inducing the elution of free  
11 proteins (including lipoproteins<sup>59, 60</sup>) using 200  $\mu\text{L}$  of 25% glycerol with 1M ammonium  
12 sulfate in PBS (300 x g, 1 min). For the protein-rich serum and milk matrices, two  
13 protein elution steps were employed to minimize protein carryover in the EV elution.  
14 Finally, the elution of the EVs was induced using 50  $\mu\text{L}$  of 50% glycerol in PBS (300 x g,  
15 1 min) and the final fraction collected. Based on the respective sample/elution volumes,  
16 a 2X concentration factor is realized.

17  
18  
19 *Quantification and characterization of EV recoveries* - Previous reports have  
20 demonstrated the validity of using standard absorbance (scattering) measurements as a  
21 means of quantifying isolated exosomes.<sup>54-56</sup> In those efforts, quantification was  
22 achieved by generating linear response curves based on serial dilutions of the  
23 commercial exosome standards in the elution solvent. Given the high complexity and  
24 presence of matrix-associated components in the diverse biofluid matrices, the method  
25 of standard addition was also used to more accurately quantify the EVs. For the  
26 method, 10  $\mu\text{L}$  of the unknown sample ( $S_0$ ) was spiked once ( $S_1$ ), twice ( $S_2$ ), and three  
27 times ( $S_3$ ) with 10  $\mu\text{L}$  of EV standards of known concentration ( $2.7 \times 10^{10}$  particles  $\text{mL}^{-1}$ ),  
28  
29  
30  
31  
32  
33  
34  
35  
36  
37  
38  
39  
40  
41  
42  
43  
44  
45  
46  
47  
48  
49  
50  
51  
52  
53  
54  
55  
56  
57  
58  
59  
60

1  
2  
3 with the total sample volumes adjusted to 50  $\mu\text{L}$  using DI-water. The absorbance of  
4  
5 each sample was measured at 203 nm ( $n=5$ ). The optical absorbance of the raw and  
6  
7 spiked samples ( $S_{0-4}$ ) and the known added concentrations of exosome standards were  
8  
9 used to create a standard addition response curve for EV quantification. The resulting  
10  
11 linear regression was extrapolated to determine the concentration of EVs in the  
12  
13 unknown sample.  
14  
15

16  
17 The structure, size, and concentration of the recovered EVs were evaluated  
18  
19 using TEM and NTA. The sample preparation for TEM imaging was performed as  
20  
21 previously reported.<sup>57</sup> The size distribution of the eluted EVs was determined using the  
22  
23 NanoSight NS300 NTA system, equipped with a 532 nm laser. Throughout NTA  
24  
25 experimentation, five replicates were collected for each sample in 60-second intervals,  
26  
27 with a minimum of 200 valid tracks recorded per video and a minimum of 1000 valid  
28  
29 tracks recorded per sample. The focal plane for each sample was manually adjusted  
30  
31 using the focus knob to achieve the best optical field of view. The syringe pump for  
32  
33 sample introduction was set to a constant flow rate of 50  $\mu\text{L}$  per minute. The camera  
34  
35 level was set to 14, and the detection threshold was set to 3, as optimized by Vestad et  
36  
37 al.<sup>66</sup> To clarify, the concentration values based on the NTA data are not the direct  
38  
39 concentration values of the EV recoveries. Instead, the recovered EVs were diluted to  
40  
41 be compatible with the NTA system's working concentration range ( $10^7$ - $10^9$  particles  
42  
43  $\text{mL}^{-1}$ ).  
44  
45  
46  
47  
48

49 Protein components of the biofluids and EV recoveries were evaluated using a  
50  
51 Bradford assay and an indirect enzyme-linked immunosorbent assay (ELISA). The  
52  
53 Bradford assay was used to determine the total protein concentration of both the whole  
54  
55  
56  
57  
58  
59  
60

1  
2  
3 samples and EV elution fractions. For the total protein determinations, 250  $\mu\text{L}$  of  
4  
5 Bradford reagent was added to 25  $\mu\text{L}$  of each sample and allowed to incubate at room  
6  
7 temperature for 20 minutes before detecting the absorbance response at 595 nm using  
8  
9 the Synergy H1 Plate Reader. The absorbance responses were compared to a standard  
10  
11 curve using BSA standards. All samples and standards were applied to the cell well  
12  
13 plate in triplicate.  
14  
15

16  
17 The presence of EVs in biofluids is commonly confirmed using antibodies to the  
18  
19 CD81, CD63, and CD9 tetraspanin proteins, which are incorporated in the  
20  
21 transmembrane space of EVs during biogenesis.<sup>67</sup> Despite their wide use as marker  
22  
23 proteins, tetraspanins are in fact not universally expressed in EVs, and the overall  
24  
25 expression is also heterogeneous among singular EV populations.<sup>68</sup> Therefore, the  
26  
27 presence of EVs may be confirmed by the detection of these proteins, but their absence  
28  
29 does not preclude the presence of EVs. Prior to chemical processing for the CD81  
30  
31 ELISA assay, the tip-isolated EVs were applied to a 100 kDa filter unit to remove latent  
32  
33 glycerol, as high concentrations of glycerol are known to interfere with antibody  
34  
35 binding.<sup>69, 70</sup> The EVs isolated from the target biofluids were first diluted in 1:1 ELISA  
36  
37 coating buffer (0.05 M carbonate-bicarbonate in PBS) and then incubated on a shaker  
38  
39 overnight at 4°C to coat the cell well plate with the analytes. An exosome standard  
40  
41 positive control and negative controls of PBS, protein elution buffer, and EV elution  
42  
43 buffer were also applied to the cell well plate. All samples and controls were applied to  
44  
45 the cell well plate in triplicate. After incubation, the cell well plates were washed with  
46  
47 sterile PBS (200  $\mu\text{L}$  per well, 30 min, 6 buffer changes) and then blocked with 5% BSA  
48  
49 in PBS at room temperature for 30 min. The wells were incubated overnight with 50  $\mu\text{L}$   
50  
51  
52  
53  
54  
55  
56  
57  
58  
59  
60

1  
2  
3 of a mouse monoclonal antibody to the CD81 protein ( $1 \mu\text{g mL}^{-1}$ ) on an orbital shaker  
4  
5 ( $4^{\circ}\text{C}$ ). The washing and blocking steps were repeated before applying  $200 \mu\text{L}$  of the  
6  
7 goat anti-mouse HRP conjugated secondary antibody ( $1 \mu\text{g mL}^{-1}$ ,  $200 \mu\text{L}$ , RT, 2 hours).  
8  
9  
10 The cell well plate was washed using  $200 \mu\text{L}$  of PBS per well and 6 buffer changes.  
11  
12 Finally, the Pierce ECL Substrate was applied and incubated at room temperature for  
13  
14 30 minutes before detection. The Synergy H1 microplate reader was used to measure  
15  
16 the chemiluminescent response resulting from the HRP catalyzed oxidation of the  
17  
18 substrate, correlating to the concentration of species containing the CD81 antigen.  
19  
20  
21

## 22 **Results and Discussion**

23  
24 *EV quantification via standard addition* - Concentrated EV recoveries with high purity,  
25  
26 preserved morphology, viability, and stability are essential for the most efficient use of  
27  
28 EVs derived *via* any isolation method. Given the complexity and diversity of the  
29  
30 biofluids (and culture media), removing matrix contaminants is of utmost importance.  
31  
32 Carryover of matrix species with the target EV isolates, including proteins and genetic  
33  
34 material, hinders the implementation of downstream characterization techniques (i.e.,  
35  
36 MS proteomics or RNA-Seq), their use in clinical analysis schemes, and use as vectors  
37  
38 in gene therapy applications. In this regard, the use of optical absorbance as an EV  
39  
40 quantification tool is particularly susceptible to interferences due to the presence of low  
41  
42 concentrations of matrix species. However, the quantification of isolated EVs by  
43  
44 absorbance has been previously demonstrated using simple optical absorbance  
45  
46 measurements at  $203 \text{ nm}$ .<sup>54-59, 61</sup> To be clear, the absorbance response observed at this  
47  
48 wavelength is not credited to the common electronic transitions typical of biomolecules  
49  
50 in solution. Instead, the “absorbance” response is caused by light scattering due to the  
51  
52  
53  
54  
55  
56  
57  
58  
59  
60

1  
2  
3 presence of the nanobodies, which is conveniently proportional to the EV concentration.  
4  
5 A cause for concern with this method for quantifying EVs is that matrix proteins and  
6  
7 nucleic acids will skew the absorbance detection, especially at the 216 and 280 nm  
8  
9 wavelengths traditionally used for determinations of proteins. These effects are  
10  
11 lessened at 203 nm, where a higher absorbance (light scattering) response is observed  
12  
13 at shorter wavelengths.<sup>48</sup> In fact, absorbance spectra obtained for EV solutions follow  
14  
15 the anticipated responses (exponentially decreasing with wavelength) for particles of  
16  
17 ~150 nm, based on Mie scattering theory.  
18  
19  
20

21 The method of standard addition is widely used for the quantification of analytes  
22  
23 whose responses (regardless of the methodology) are subjected to significant matrix  
24  
25 interferences.<sup>71</sup> The method has not been previously employed for the quantification of  
26  
27 EVs in biofluids, but could prove useful in this application as diverse matrices are being  
28  
29 evaluated. A proof of concept for this method is illustrated in Fig. 2, where the method of  
30  
31 standard addition was used to quantify EVs in aqueous solution using the commercial  
32  
33 exosome stock. The method was first applied to test the “unknown”, which was the  
34  
35 initial exosome stock solution of  $7.0 \times 10^{10}$  particles  $\text{mL}^{-1}$ . The test unknown ( $S_0$ ) was  
36  
37 spiked once ( $S_1$ ), twice ( $S_2$ ), and three times ( $S_3$ ) with aqueous aliquots of the EV  
38  
39 standard, increasing the theoretical concentrations by  $1.1 \times 10^{10}$ ,  $2.2 \times 10^{10}$ , and  $3.2 \times$   
40  
41  $10^{10}$  particles  $\text{mL}^{-1}$ , respectively. As shown in Fig. 2 (red line), the absorbance  
42  
43 responses for the un-spiked ( $S_0$ ) and spiked ( $S_1$ ,  $S_2$ ,  $S_3$ ) EV stock aliquots in DI-water  
44  
45 are well behaved, yielding a correlation coefficient ( $R^2$ ) of  $>0.999$ . Based on the linear  
46  
47 regression, the “unknown” concentration was determined to be  $7.4 \times 10^{10}$  particles  $\text{mL}^{-1}$ ,  
48  
49 a 5% error. As a point of reference, the concentration of the same solution determined  
50  
51  
52  
53  
54  
55  
56  
57  
58  
59  
60

1  
2  
3 by a standard calibration curve ( $R^2$ -value = 0.998) yielded a concentration of  $6.3 \times 10^{10}$   
4 particles  $\text{mL}^{-1}$ , a 10% error (accuracy that would be considered outstanding by virtually  
5 any other EV assay method).  
6  
7  
8  
9

10 As mentioned previously, the stock exosome material is known to contain  
11 undetermined amounts of proteinaceous material and other vesicular bodies. As a  
12 further test of the use of the standard addition quantification method, the “unknown”  
13 sample and the equivalent spike samples were put through the spin-down protocol. As  
14 seen in the response curve (blue line), proportional recoveries are indeed maintained,  
15 reflecting a lack of any sort of overloading of the fiber phase. Indeed, the recoveries are  
16 quite high versus the EVs in the stock aqueous solution, ranging from 96-102%  
17 (concentration of recovered EVs /raw stock), with the lower y-intercept being attributed  
18 to the removal of the latent proteins in the original stock material. Also of relevance, the  
19 average variation for the bulk measurements was 4 %RSD, while for the full extraction  
20 process the variability averaged 5 %RSD. There is some level of degraded quantitative  
21 performance (scatter) in the tip recoveries, as seen in the lessened goodness-of-fit ( $R^2$   
22 = 0.970).  
23  
24  
25  
26  
27  
28  
29  
30  
31  
32  
33  
34  
35  
36  
37  
38  
39

40 *EV recoveries from diverse matrices* - After confirming the ability of the standard  
41 addition method to determine the concentration of EVs and the C-CP tip’s ability to  
42 produce quantitative EV recoveries, the experimental protocol was applied to the raw  
43 biofluid matrices. The urine, saliva, cervical mucus, serum, and milk biofluids samples  
44 were spiked as described above, followed by tip isolation. The raw biofluids were spiked  
45 once, twice, and three times with EV stock solutions of increasing concentration ( $1.1 \times$   
46  $10^{10}$  particles  $\text{mL}^{-1}$  per spike), then diluted to 200  $\mu\text{L}$  with ammonium sulfate (2M final  
47  
48  
49  
50  
51  
52  
53  
54  
55  
56  
57  
58  
59  
60



1  
2  
3 concentration) before applying to the C-CP spin-down tips for the isolation process  
4  
5 (load, protein wash, EV elution). The absorbance response of the EV eluates was  
6  
7 measured at 203 nm. The relative absorbance responses presented in Fig. 3 reflect the  
8  
9 fact that the C-CP tip does produce EV recoveries of proportionally increasing  
10  
11 concentrations, despite the biofluid sample complexity. The respective regressions of  
12  
13 each have an  $R^2$  correlation coefficient of  $>0.98$ . The determined values for each of the  
14  
15 biofluids are provided in each case, with respective values each falling in line with  
16  
17 expectations based on literature values.<sup>72-76</sup> The relative precision of the determined  
18  
19 values ( $n=3$ ) is excellent, with an average value of  $\sim 7$  %RSD across the matrices.  
20  
21  
22  
23

24 The relative responses for the spikes across the different matrices are  
25  
26 fundamentally instructive. In theory, consecutive increases of  $1.1 \times 10^{10}$  particles  $\text{mL}^{-1}$   
27  
28 EV concentration were applied. Therefore, given a homogenous and ideal biofluid  
29  
30 sample, the difference between the determined concentrations of the  $S_x$  and  $S_{x+n}$   
31  
32 samples should be  $1.1 \times 10^{10}$  particles per mL. While the responses here are  
33  
34 proportional within each matrix type, there is a definitive difference in the slopes; i.e. the  
35  
36 method of standard addition reveals the existence of matrix effects. That said, given  
37  
38 the vast physico-chemical differences among these biofluids, the extent of the effects,  
39  
40 based on the slopes of the response curves, are less than a factor of 2x. As such, the  
41  
42 use of a single absorbance calibration function would deliver that level of accuracy, with  
43  
44 higher levels achieved with the use of matrix-matched standards. Analysis across  
45  
46 multiple matrices would benefit most using the standard addition method.  
47  
48  
49  
50

51  
52 *Physical characterization of EV isolates* - To confirm that the C-CP tip elution fractions  
53  
54 do indeed contain EVs in the correct size range and consist of the expected  
55  
56  
57  
58  
59  
60

1  
2  
3 characteristic shape, NTA and TEM imaging were performed. Figure 4 presents both  
4 the size distributions observed via NTA and electron micrographs of the intact vesicles  
5 following isolation. The eluted EVs presented average diameters from 121.7-160.3 nm  
6 across the matrices. Based on the NTA data, the populations of EVs recovered from the  
7 urine, saliva, and milk samples presented the most “gaussian-like” size distributions,  
8 though with minor subsets of vesicles detected at larger sizes (as is typical). On the  
9 other hand, the EVs isolated from the cervical mucus and blood serum samples were  
10 far less homogeneous, with several distinct subpopulations.  
11  
12  
13  
14  
15  
16  
17  
18  
19  
20

21 Visualization via transmission electron microscopy (TEM) is another benchmark  
22 method to identify extracellular vesicles. The TEM micrographs presented in Fig. 4  
23 confirm that EVs were isolated from the biofluids using the C-CP spin-down tips. In each  
24 of the images, either cup-shaped, donut-shaped, or spherical-shaped vesicles with a  
25 dark halo can be observed. The EVs observed in the TEM micrographs fall within the  
26 exosome size range. One key aspect to emphasize is that, even in the potentially  
27 lipoprotein-heavy biofluids (cervical mucus, serum, milk), no vesicles are observed that  
28 would correspond to the anticipated lipoprotein size range (~20 nm) characteristic of  
29 LDLs. The isolation of EVs from lipoproteins is a fundamental challenge due to the  
30 similarities of the vesicles’ size, structure, composition, and biological interactions.<sup>40, 41</sup>  
31 High purity recovery of EVs (i.e., the lack of matrix proteins/lipoproteins) using the fiber  
32 isolation methodology has been demonstrated in recent mass spectrometric proteomics  
33 analyses,<sup>59, 60</sup> and is a significant advantage of the C-CP tip isolation technique. This  
34 point is further demonstrated in the following section. The TEM images show that the  
35  
36  
37  
38  
39  
40  
41  
42  
43  
44  
45  
46  
47  
48  
49  
50  
51  
52  
53  
54  
55  
56  
57  
58  
59  
60

1  
2  
3 HIC-based C-CP tip isolation preserves the characteristic vesicular shape with no visual  
4  
5 contamination.  
6  
7

8           Beyond the size distribution, NTA can also be used as a semi-quantitative means  
9  
10 of determining nanoparticle densities. As presented in Fig. 5a, the particle densities  
11  
12 determined for the raw biofluids via NTA can be appreciably higher than the  
13  
14 corresponding values generated by absorbance measurements. Not surprisingly, this is  
15  
16 particularly true for the most proteinaceous matrices (where agglomeration would likely  
17  
18 occur). In these cases, the densities determined by NTA can exceed those of  
19  
20 absorbance by as much as an order of magnitude, with the measurement variability also  
21  
22 highest for those samples. Importantly, the same analyses performed on the spin-down  
23  
24 isolates (Fig. 5b) yield values in far better agreement between the two quantification  
25  
26 methods, with much-improved measurement precision realized for the NTA. It is  
27  
28 noteworthy that the relative concentrations across the matrices parallel each other  
29  
30 between the two independent measurement methods, with the values not differing by  
31  
32 more than 2x. This level of agreement is seen as validation of the efficacy of the C-CP  
33  
34 fiber spin-down tip methodology.  
35  
36  
37  
38  
39

40 *Characterization of EV purity* - To investigate the purity of EVs (based on the removal  
41  
42 of matrix proteins) isolated using the C-CP tip method, a Bradford assay was  
43  
44 performed. The total protein concentrations of the whole biofluid samples and the EVs  
45  
46 eluted from those biofluids using the C-CP tip isolation method were determined. To be  
47  
48 clear, a Bradford assay reflects the total proteinaceous material present in a sample.  
49  
50 As such, in the ideal case of perfect isolation of EVs, a positive response will still result  
51  
52 due to the interaction between the Bradford reagent and surface proteins and externally  
53  
54  
55  
56  
57  
58  
59  
60

1  
2  
3 exposed basic and aromatic amino acid residues. The Bradford assay results for the  
4 raw matrix materials and the EV isolates are presented in Fig. 6. As would be  
5 anticipated, the goat milk and human blood serum matrices were the most protein-  
6 dense, with the human urine matrix having the lowest amount of protein present. After  
7 conducting the C-CP fiber spin-down tip EV isolation workflow, most of the  
8 contaminating proteins were removed while leaving behind the EVs, which contribute to  
9 only a small fraction of the total protein response for the protein-rich matrices. Here, the  
10 67-89% removal of “total protein” was demonstrated for the saliva, cervical mucus,  
11 serum, and milk biofluid samples. A much lower (17%) removal of proteins was  
12 observed from the human urine sample, as expected given the much lower relative  
13 concentration of free protein in healthy urine samples. The EV recoveries present a low  
14 (346-412  $\mu\text{g mL}^{-1}$ ) total protein concentration based on the Bradford assay. While not  
15 perceivable on this scale, the relative amounts of determined protein for the isolates are  
16 a very close reflection of their relative EV densities determined via the standard addition  
17 and NTA methods (Figs. 3 and 5), suggesting the efficacy of the method to yield high-  
18 purity EVs. The C-CP tip method demonstrates here the ability to remove up to 89% of  
19 protein contaminant species. The efficiency of the method is demonstrated by the  
20 absence of proteinaceous aggregates in the TEM micrographs of EVs after the tip  
21 isolation process. Perhaps most definitive, recent MS proteomic analysis work has  
22 confirmed the removal of common contaminant lipoprotein species from serum samples  
23 using this method, based on the virtual absence (<0.3% of total proteins) of the Apo-  
24 B100 content in the EV isolates.<sup>60</sup> The depletion of the lipid marker protein was  
25 confirmed by ELISA analysis, as well.<sup>60</sup>  
26  
27  
28  
29  
30  
31  
32  
33  
34  
35  
36  
37  
38  
39  
40  
41  
42  
43  
44  
45  
46  
47  
48  
49  
50  
51  
52  
53  
54  
55  
56  
57  
58  
59  
60

1  
2  
3 *Verification of EV identity* - While no universally expressed EV/exosome marker exists,  
4  
5 the CD81 tetraspanin protein has been identified in high concentrations in many  
6  
7 exosome populations.<sup>55</sup> (The CD63 and CD9 tetraspanins have been used as  
8  
9 identifiers in previous works from this laboratory,<sup>57</sup> but CD81 generally exists in higher  
10  
11 concentrations.) As such, the marker has been accepted as a general marker for the  
12  
13 presence of EVs, with the acknowledgment that it is expressed to different extents even  
14  
15 within the same EV population, and in some cases not at all. To confirm the presence  
16  
17 of EVs in the C-CP tip eluates and assess the recovered vesicles' bioactivity, a semi-  
18  
19 quantitative ELISA using an antibody to the CD81 tetraspanin protein was employed.  
20  
21 As shown in Fig. 7, serial dilutions of the commercial exosome standard stock were  
22  
23 used to create a standard curve for the ELISA response quantification. With this  
24  
25 standard curve of linear response ( $R^2 = 0.985$ ), the concentration of recovered EVs  
26  
27 containing the CD81 tetraspanin protein was estimated. When the concentration of EV  
28  
29 standards presenting a CD81 response was compared to the EV concentration as  
30  
31 determined by absorbance detection (Fig. 3), the relative concentrations show the same  
32  
33 general trends among the matrices. Even so, the quantitative numbers for the exosome  
34  
35 concentrations reflect recoveries of 53-91% across the matrix types versus the  
36  
37 absorbance-determined concentrations (Fig. 3). This level of agreement between the  
38  
39 highly generic (absorbance) and highly specific (ELISA) means of quantification is quite  
40  
41 remarkable. Based solely on the CD81 ELISA, the highest percentage of recovery for  
42  
43 EVs containing CD81 was found for the blood serum sample (91%), followed by the  
44  
45 saliva (70%), urine (59%), cervical mucus (58%), and the goat milk (53%). This level of  
46  
47  
48  
49  
50  
51  
52  
53  
54  
55  
56  
57  
58  
59  
60

1  
2  
3 variation is not at all surprising because CD81 is not universally expressed and is  
4  
5 upregulated/downregulated in EVs of different origins.  
6  
7

## 8 **Conclusions**

9

10 The C-CP fiber tip isolation method has proven to be an efficient means of EV  
11 isolation, with the ability to withstand potentially complex matrix effects from human  
12 urine, saliva, cervical mucus, blood serum, and goat milk. The HIC-based EV isolation  
13 technique presents significant benefits regarding time, cost, and ease of use. The C-CP  
14 spin-down tip workflow enables the processing of multiple samples simultaneously in 15  
15 min, limited only by the table-top centrifuge capacity. The method of standard addition  
16 employing a commercial exosome standard stock was demonstrated as an accurate  
17 means to determine the concentration of EVs, regardless of the matrix type. That said,  
18 the respective responses showed very little difference in sensitivity (i.e., minimal matrix  
19 effects). NTA analysis provided the determination of particle size distributions and  
20 overall particle densities for the different matrices. TEM analysis confirms that the EVs  
21 isolated from all biofluids retained the characteristic cup or donut-shaped morphology  
22 after the isolation process. The purity of the EV isolates was confirmed through Bradford  
23 assays, revealing total protein content before and after isolation, with up to 89% of  
24 biofluid-originating proteins being removed. The efficacy of the method to isolate  
25 bioactive EVs was demonstrated through an ELISA assay for the CD81 tetraspanin  
26 marker protein. Overall, there was a self-consistency in the relative (and absolute)  
27 amounts of EVs isolated from the different matrices based on the multiple, independent  
28 measurement approaches. This agreement serves to validate the quantitative aspects  
29 of the isolation process.  
30  
31  
32  
33  
34  
35  
36  
37  
38  
39  
40  
41  
42  
43  
44  
45  
46  
47  
48  
49  
50  
51  
52  
53  
54  
55  
56  
57  
58  
59  
60

1  
2  
3           The bench-top C-CP spin-down tip protocol introduces a relatively facile means  
4  
5 of EV isolation. The C-CP tip HIC isolation method's capabilities make it an ideal  
6  
7 candidate for use in laboratory settings. The ability to work with microliter volumes  
8  
9 while achieving high EV yields and purity lends itself to both clinical and fundamental  
10  
11 EV research applications. For example, the ability to alleviate the complicating aspects  
12  
13 of serum/lipoproteins is an essential element in performing high-fidelity proteomics  
14  
15 analysis. Likewise, the same factors are key in developing bioassays based on the  
16  
17 presence of targeted surface marker proteins. Finally, while likely requiring the use of  
18  
19 preparative scale columns, the characteristics demonstrated here are essential in the  
20  
21 development of EVs as gene therapy vectors.  
22  
23  
24  
25  
26  
27  
28

### 29   **Conflicts of interest/Competing interests**

30  
31           The authors declare no conflicts of interest.  
32  
33  
34  
35

### 36   **Acknowledgments**

37  
38           Financial support for the chromatography development efforts came from the National  
39  
40 Science Foundation, Division of Chemistry under grant CHE-1608663. Financial support  
41  
42 for the EV and exosome isolation efforts came from the Eppley Foundation for Scientific  
43  
44 Research and The Gibson Foundation. Dr. Larry Puls (Prisma Health), the Prisma  
45  
46 Health ITOR Biorepository, and Prisma Health are gratefully acknowledged for patient  
47  
48 identification and sample collection. Special thanks to George Wetzel, Clemson  
49  
50 University Electron Microscopy Facility for assistance with EM. The content of this  
51  
52 material and any opinions, findings, conclusions, or recommendations expressed in this  
53  
54  
55  
56  
57  
58  
59  
60

1  
2  
3 material are solely the responsibility of the author(s) and do not necessarily represent  
4 the official views of the National Science Foundation. The graphical abstract presented  
5 here was created with BioRender.com.  
6  
7  
8  
9  
10  
11  
12  
13

#### 14 **CRedit Authorship contribution statement**

15  
16 **Kaylan K. Jackson:** Methodology, Data Curation, Visualization, Writing – Original Draft  
17 Preparation; **Rhonda R. Powell:** Methodolog; **Terri F. Bruce:** Conceptualization,  
18 Supervision; **R. Kenneth Marcus:** Conceptualization, Supervision, Writing – Reviewing  
19 and Editing  
20  
21  
22  
23  
24  
25  
26  
27  
28  
29  
30  
31  
32  
33  
34  
35  
36  
37  
38  
39  
40  
41  
42  
43  
44  
45  
46  
47  
48  
49  
50  
51  
52  
53  
54  
55  
56  
57  
58  
59  
60



## References

1. F. Momen-Heravi, L. Balaj, S. Alian, P.-Y. Mantel, A. E. Halleck, A. J. Trachtenberg, C. E. Soria, S. Oquin, C. M. Bonebreak and E. Saracoglu, *Biol. Chem.*, 2013, **394**, 1253-1262.
2. F. M. Heravi, S. Bala, K. Kodys and G. Szabo, *Sci. Rep.*, 2015, **5**, 9991.
3. Y. Ouyang, A. Bayer, T. Chu, V. A. Tyurin, V. E. Kagan, A. E. Morelli, C. B. Coyne and Y. Sadovsky, *Placenta*, 2016, **47**, 86-95.
4. S. Keerthikumar, D. Chisanga, D. Ariyaratne, H. Al Saffar, S. Anand, K. Zhao, M. Samuel, M. Pathan, M. Jois, N. Chilamkurti, L. Gangoda and S. Mathivanan, *J. Mol. Biol.*, 2016, **428**, 688-692.
5. S. Pant, H. Hilton and M. E. Burczynski, *Biochem. Pharmacol.*, 2012, **83**, 1484-1494.
6. Z. J. Smith, C. Lee, T. Rojalin, R. P. Carney, S. Hazari, A. Knudson, K. Lam, H. Saari, E. L. Ibanez, T. Viitala, T. Laaksonen, M. Yliperttula and S. Wachsmann-Hogiu, *J. Extracell. Vesicles*, 2015, **4**, 28533.
7. K. L. Schey, J. M. Luther and K. L. Rose, *Methods*, 2015, **87**, 75-82.
8. M. Colombo, C. Moita, G. van Niel, J. Kowal, J. Vigneron, P. Benaroch, N. Manel, L. F. Moita, C. Thery and G. Raposo, *J. Cell Sci.*, 2013, **126**, 5553-5565.
9. J. Kowal, M. Tkach and C. Théry, *Curr. Opin. Cell Biol.*, 2014, **29**, 116-125.
10. M. Kanada, M. H. Bachmann and C. H. Contag, *Trends Cancer*, 2016, **2**, 84-94.
11. V. Sokolova, A. K. Ludwig, S. Hornung, O. Rotan, P. A. Horn, M. Epple and B. Giebel, *Colloid Surf. B*, 2011, **87**, 146-150.
12. E. Willms, H. J. Johansson, I. Mager, Y. Lee, K. E. M. Blomberg, M. Sadik, A. Alaarg, C. I. E. Smith, J. Lehtio, S. E. L. Andaloussi, M. J. A. Wood and P. Vader, *Scientific Reports*, 2016, **6**, 12.
13. A. Bobrie, M. Colombo, S. Krumeich, G. Raposo and C. Thery, *J. Extracell. Vesicles*, 2012, **1**, 18397.
14. A. Bobrie, M. Colombo, G. Raposo and C. Thery, *Traffic (Copenhagen, Denmark)*, 2011, **12**, 1659-1668.
15. A. V. Vlassov, S. Magdaleno, R. Setterquist and R. Conrad, *Biochim. Biophys. Acta*, 2012, **1820**, 940-948.
16. S. Roy, F. H. Hochberg and P. S. Jones, *J. Extracell. Vesicles*, 2018, **7**, 1438720.
17. D. M. Pegtel and S. J. Gould, *Ann. Rev. Biochem.*, 2019, **88**, 487-514.
18. L. L. Yu, J. Zhu, J. X. Liu, F. Jiang, W. K. Ni, L. S. Qu, R. Z. Ni, C. H. Lu and M. B. Xiao, *Biomed. Res. Int.*, 2018, **2018**, 3634563.
19. S. Halvaei, S. Daryani, Z. Eslami-S, T. Samadi, N. Jafarbeik-Iravani, T. O. Bakhshayesh, K. Majidzadeh-A and R. Esmaeili, *Mol. Ther. - Nucl. Acids*, 2018, **10**, 131-141.
20. K. B. Johnsen, J. M. Gudbergsson, M. N. Skov, L. Pilgaard, T. Moos and M. Duroux, *Biochim. Biophys. Acta*, 2014, **1846**, 75-87.
21. R. C. Lai, F. Arslan, M. M. Lee, N. S. K. Sze, A. Choo, T. S. Chen, M. Salto-Tellez, L. Timmers, C. N. Lee, R. M. El Oakley, G. Pasterkamp, D. P. V. de Kleijn and S. K. Lim, *Stem Cell Res.*, 2010, **4**, 214-222.
22. X. Yang, Z. Weng, D. L. Mendrick and Q. Shi, *Toxicol. Lett.*, 2014, **225**, 401-406.

23. M. L. Merchant, I. M. Rood, J. K. J. Deegens and J. B. Klein, *Nat. Rev. Nephrol.*, 2017, **13**, 731-749.
24. J. Q. Gerlach, A. Kruger, S. Gallogly, S. A. Hanley, M. C. Hogan, C. J. Ward, L. Joshi and M. D. Griffin, *PLoS One*, 2013, **8**, e74801.
25. C. Lasser, V. S. Alikhani, K. Ekstrom, M. Eldh, P. T. Paredes, A. Bossios, M. Sjostrand, S. Gabrielsson, J. Lotvall and H. Valadi, *J. Transl. Med.*, 2011, **9**, 9.
26. L. A. Aqrawi, H. K. Galtung, B. Vestad, R. Øvstebø, B. Thiede, S. Rusthen, A. Young, E. M. Guerreiro, T. P. Utheim and X. Chen, *Arthritis Res. Ther.*, 2017, **19**, 14.
27. F. V. Winck, A. C. Prado Ribeiro, R. Ramos Domingues, L. Y. Ling, D. M. Riano-Pachon, C. Rivera, T. B. Brandao, A. F. Gouvea, A. R. Santos-Silva, R. D. Coletta and A. F. Paes Leme, *Sci. Rep.*, 2015, **5**, 16305.
28. B. Pang, Y. Zhu, J. Ni, J. Ruan, J. Thompson, D. Malouf, J. Bucci, P. Graham and Y. Li, *Int. J. Nanomedicine*, 2020, **15**, 10241-10256.
29. T. Shtam, S. Naryzhny, A. Kopylov, E. Petrenko, R. Samsonov, R. Kamyshinsky, Y. Zabrodskaaya, D. Nikitin, M. Sorokin, A. Buzdin and A. Malek, *J. Hematol.*, 2018, **7**, 149-153.
30. X. Zhao, Y. Wu, J. Duan, Y. Ma, Z. Shen, L. Wei, X. Cui, J. Zhang, Y. Xie and J. Liu, *J. Proteome Res.*, 2014, **13**, 5391-5402.
31. K. Blans, M. S. Hansen, L. V. Sorensen, M. L. Hvam, K. A. Howard, A. Moller, L. Wiking, L. B. Larsen and J. T. Rasmussen, *J. Extracell. Vesicles*, 2017, **6**, 1294340.
32. M. I. Zonneveld, A. R. Brisson, M. J. van Herwijnen, S. Tan, C. H. van de Lest, F. A. Redegeld, J. Garssen, M. H. Wauben and E. N. Nolte-'t Hoen, *J. Extracell. Vesicles*, 2014, **3**, 24215.
33. Y. K. Yoo, J. Lee, H. Kim, K. S. Hwang, D. S. Yoon and J. H. Lee, *Micromachines-Basel*, 2018, **9**, 634.
34. D. Chiasserini, J. R. van Weering, S. R. Piersma, T. V. Pham, A. Malekzadeh, C. E. Teunissen, H. de Wit and C. R. Jimenez, *J. Proteomics*, 2014, **106**, 191-204.
35. A. Milasan, N. Tessandier, S. Tan, A. Brisson, E. Boilard and C. Martel, *J. Extracell. Vesicles*, 2016, **5**, 31427.
36. N. Tessandier, I. Melki, N. Cloutier, I. Allaey, A. Miszta, S. Tan, A. Milasan, S. Michel, A. Benmoussa, T. Levesque, F. Cote, S. E. McKenzie, C. Gilbert, P. Provost, A. R. Brisson, A. S. Wolberg, P. R. Fortin, C. Martel and E. Boilard, *Arterioscler. Thromb. Vasc. Biol.*, 2020, **40**, 929-942.
37. E. I. Buzas, B. Gyorgy, G. Nagy, A. Falus and S. Gay, *Nat. Rev. Rheumatol.*, 2014, **10**, 356-364.
38. C. Balbi, M. Piccoli, L. Barile, A. Papait, A. Armirotti, E. Principi, D. Reverberi, L. Pascucci, P. Becherini, L. Varesio, M. Mogni, D. Coviello, T. Bandiera, M. Pozzobon, R. Cancedda and S. Bollini, *Stem Cells Transl. Med.*, 2017, **6**, 1340-1355.
39. C. Gardiner, D. Di Vizio, S. Sahoo, C. Thery, K. W. Witwer, M. Wauben and A. F. Hill, *J. Extracell. Vesicles*, 2016, **5**, 32945.
40. J. B. Simonsen, *Circ. Res.*, 2017, **121**, 920-922.

- 1  
2  
3 41. B. W. Sódar, Á. Kittel, K. Pálóczi, K. V. Vukman, X. Osteikoetxea, K. Szabó-  
4 Taylor, A. Németh, B. Sperlágh, T. Baranyai and Z. Giricz, *Sci. Rep.*, 2016, **6**,  
5 24316-24327.  
6  
7 42. C. Thery, K. W. Witwer, E. Aikawa, M. J. Alcaraz, J. D. Anderson, R.  
8 Andriantsitohaina, A. Antoniou, T. Arab, F. Archer, G. K. Atkin-Smith, D. C. Ayre,  
9 J. M. Bach, D. Bachurski, H. Baharvand, L. Balaj, S. Baldacchino, N. N. Bauer,  
10 A. A. Baxter, M. Bebawy, C. Beckham, A. B. Zavec, A. Benmoussa, A. C.  
11 Berardi, P. Bergese, E. Bielska, C. Blenkiron, S. Bobis-Wozowicz, E. Boilard, W.  
12 Boireau, A. Bongiovanni, F. E. Borrás, S. Bosch, C. M. Boulanger, X.  
13 Breakefield, A. M. Breglio, M. A. Brennan, D. R. Brigstock, A. Brisson, M. L. D.  
14 Broekman, J. F. Bromberg, P. Bryl-Gorecka, S. Buch, A. H. Buck, D. Burger, S.  
15 Busatto, D. Buschmann, B. Bussolati, E. I. Buzas, J. B. Byrd, G. Camussi, D. R.  
16 F. Carter, S. Caruso, L. W. Chamley, Y. T. Chang, C. C. Chen, S. Chen, L.  
17 Cheng, A. R. Chin, A. Clayton, S. P. Clerici, A. Cocks, E. Cocucci, R. J. Coffey,  
18 A. Cordeiro-da-Silva, Y. Couch, F. A. W. Coumans, B. Coyle, R. Crescitelli, M. F.  
19 Criado, C. D'Souza-Schorey, S. Das, A. D. Chaudhuri, P. de Candia, E. F. De  
20 Santana, O. De Wever, H. A. del Portillo, T. Demaret, S. Deville, A. Devitt, B.  
21 Dhondt, D. Di Vizio, L. C. Dieterich, V. Dolo, A. P. D. Rubio, M. Dominici, M. R.  
22 Dourado, T. A. P. Driedonks, F. V. Duarte, H. M. Duncan, R. M. Eichenberger, K.  
23 Ekstrom, S. E. L. Andaloussi, C. Elie-Caille, U. Erdbrugger, J. M. Falcon-Perez,  
24 F. Fatima, J. E. Fish, M. Flores-Bellver, A. Forsonits, A. Frelet-Barrand, F. Fricke,  
25 G. Fuhrmann, S. Gabrielsson, A. Gamez-Valero, C. Gardiner, K. Gartner, R.  
26 Gaudin, Y. S. Gho, B. Giebel, C. Gilbert, M. Gimona, I. Giusti, D. C. I.  
27 Goberdhan, A. Gorgens, S. M. Gorski, D. W. Greening, J. C. Gross, A. Gualerzi,  
28 G. N. Gupta, D. Gustafson, A. Handberg, R. A. Haraszti, P. Harrison, H. Hegyesi,  
29 A. Hendrix, A. F. Hill, F. H. Hochberg, K. F. Hoffmann, B. Holder, H. Holthofer, B.  
30 Hosseinkhani, G. K. Hu, Y. Y. Huang, V. Huber, S. Hunt, A. G. E. Ibrahim, T.  
31 Ikezu, J. M. Inal, M. Isin, A. Ivanova, H. K. Jackson, S. Jacobsen, S. M. Jay, M.  
32 Jayachandran, G. Jenster, L. Z. Jiang, S. M. Johnson, J. C. Jones, A. Jong, T.  
33 Jovanovic-Talisman, S. Jung, R. Kalluri, S. Kano, S. Kaur, Y. Kawamura, E. T.  
34 Keller, D. Khamari, E. Khomyakova, A. Khvorova, P. Kierulf, K. P. Kim, T.  
35 Kislinger, M. Klingeborn, D. J. Klinke, M. Kornek, M. M. Kosanovic, A. F. Kovacs,  
36 E. M. Kramer-Albers, S. Krasemann, M. Krause, I. V. Kurochkin, G. D. Kusuma,  
37 S. Kuypers, S. Laitinen, S. M. Langevin, L. R. Languino, J. Lannigan, C. Lasser,  
38 L. C. Laurent, G. Lavieu, E. Lazaro-Ibanez, S. Le Lay, M. S. Lee, Y. X. F. Lee, D.  
39 S. Lemos, M. Lenassi, A. Leszczynska, I. T. S. Li, K. Liao, S. F. Libregts, E.  
40 Ligeti, R. Lim, S. K. Lim, A. Line, K. Linnemannstons, A. Llorente, C. A. Lombard,  
41 M. J. Lorenowicz, A. M. Lorincz, J. Lotvall, J. Lovett, M. C. Lowry, X. Loyer, Q.  
42 Lu, B. Lukomska, T. R. Lunavat, S. L. N. Maas, H. Malhi, A. Marcilla, J. Mariani,  
43 J. Mariscal, E. S. Martens-Uzunova, L. Martin-Jaular, M. C. Martinez, V. R.  
44 Martins, M. Mathieu, S. Mathivanan, M. Maugeri, L. K. McGinnis, M. J. McVey, D.  
45 G. Meckes, K. L. Meehan, I. Mertens, V. R. Minciacci, A. Moller, M. M.  
46 Jorgensen, A. Morales-Kastresana, J. Morhayim, F. Mullier, M. Muraca, L.  
47 Musante, V. Mussack, D. C. Muth, K. H. Myburgh, T. Najrana, M. Nawaz, I.  
48 Nazarenko, P. Nejsun, C. Neri, T. Neri, R. Nieuwland, L. Nimrichter, J. P. Nolan,  
49 E. N. M. Nolte-'t Hoen, N. Noren Hooten, L. O'Driscoll, T. O'Grady, A. O'Loghlen,  
50  
51  
52  
53  
54  
55  
56  
57  
58  
59  
60

- 1  
2  
3 T. Ochiya, M. Olivier, A. Ortiz, L. A. Ortiz, X. Osteikoetxea, O. Ostegaard, M.  
4 Ostrowski, J. Park, D. M. Pegtel, H. Peinado, F. Perut, M. W. Pfaffl, D. G.  
5 Phinney, B. C. H. Pieters, R. C. Pink, D. S. Pisetsky, E. P. von Strandmann, I.  
6 Polakovicova, I. K. H. Poon, B. H. Powell, I. Prada, L. Pulliam, P. Quesenberry,  
7 A. Radeghieri, R. L. Raffai, S. Raimondo, J. Rak, M. I. Ramirez, G. Raposo, M.  
8 S. Rayyan, N. Regev-Rudzki, F. L. Ricklefs, P. D. Robbins, D. D. Roberts, S. C.  
9 Rodrigues, E. Rohde, S. Rome, K. M. A. Rouschop, A. Ruggetti, A. E. Russell, P.  
10 Saa, S. Sahoo, E. Salas-Huenuleo, C. Sanchez, J. A. Saugstad, M. J. Saul, R.  
11 M. Schiffelers, R. Schneider, T. H. Schoyen, A. Scott, E. Shahaj, S. Sharma, O.  
12 Shatnyeva, F. Shekari, G. V. Shelke, A. K. Shetty, K. Shiba, P. R. M. Siljander,  
13 A. M. Silva, A. Skowronek, O. L. Snyder, R. P. Soares, B. W. Sodar, C.  
14 Soekmadji, J. Sotillo, P. D. Stahl, W. Stoorvogel, S. L. Stott, E. F. Strasser, S.  
15 Swift, H. Tahara, M. Tewari, K. Timms, S. Tiwari, R. Tixeira, M. Tkach, W. S.  
16 Toh, R. Tomasini, A. C. Torrecilhas, J. P. Tosar, V. Toxavidis, L. Urbanelli, P.  
17 Vader, B. W. M. van Balkom, S. G. van der Grein, J. Van Deun, M. J. C. van  
18 Herwijnen, K. Van Keuren-Jensen, G. van Niel, M. E. van Royen, A. J. van  
19 Wijnen, M. H. Vasconcelos, I. J. Vechetti, T. D. Veit, L. J. Vella, E. Velot, F. J.  
20 Verweij, B. Vestad, J. L. Vinas, T. Visnovitz, K. V. Vukman, J. Wahlgren, D. C.  
21 Watson, M. H. M. Wauben, A. Weaver, J. P. Webber, V. Weber, A. M. Wehman,  
22 D. J. Weiss, J. A. Welsh, S. Wendt, A. M. Wheelock, Z. Wiener, L. Witte, J.  
23 Wolfram, A. Xagorari, P. Xander, J. Xu, X. M. Yan, M. Yanez-Mo, H. Yin, Y.  
24 Yuana, V. Zappulli, J. Zarubova, V. Zekas, J. Y. Zhang, Z. Z. Zhao, L. Zheng, A.  
25 R. Zheutlin, A. M. Zickler, P. Zimmermann, A. M. Zivkovic, D. Zocco and E. K.  
26 Zuba-Surma, *J. Extracell. Vesicles*, 2018, **7**, 43.  
27  
28 43. T. Liangsupree, E. Multia and M.-L. Riekkola, *J. Chromatogr. A*, 2021, **1636**,  
29 461773.  
30  
31 44. K. W. Witwer, C. Soekmadji, A. F. Hill, M. H. Wauben, E. I. Buzás, D. Di Vizio, J.  
32 M. Falcon-Perez, C. Gardiner, F. Hochberg, I. V. Kurochkin, J. Lötval, S.  
33 Mathivanan, R. Nieuwland, S. Sahoo, H. Tahara, A. C. Torrecilhas, A. M.  
34 Weaver, H. Yin, L. Zheng, Y. S. Ghossein, P. Quesenberry and C. Théry, *J. Extracell.*  
35 *Vesicles*, 2017, **6**, 1396823.  
36  
37 45. M. Macias, V. Rebmann, B. Mateos, N. Varo, J. L. Perez-Gracia, E. Alegre and  
38 A. Gonzalez, *Clin. Chem. Lab. Med.*, 2019, **57**, 1539-1545.  
39  
40 46. Y. Yuana, J. Levels, A. Grootemaat, A. Sturk and R. Nieuwland, *J. Extracell.*  
41 *Vesicles*, 2014, **3**, 23262.  
42  
43 47. B. J. Tauro, D. W. Greening, R. A. Mathias, H. Ji, S. Mathivanan, A. M. Scott and  
44 R. J. Simpson, *Methods*, 2012, **56**, 293-304.  
45  
46 48. D. Freitas, M. Balmaña, J. Poças, D. Campos, H. Osório, A. Konstantinidi, S. Y.  
47 Vakhrushev, A. Magalhães and C. A. Reis, *J. Extracell. Vesicles*, 2019, **8**,  
48 1621131.  
49  
50 49. G. Vergauwen, B. Dhondt, J. Van Deun, E. De Smedt, G. Berx, E. Timmerman,  
51 K. Gevaert, I. Miinalainen, V. Cocquyt, G. Braems, R. Van den Broecke, H.  
52 Denys, O. De Wever and A. Hendrix, *Sci. Rep.*, 2017, **7**, 2704.  
53  
54 50. A. Gámez-Valero, M. Monguió-Tortajada, L. Carreras-Planella, M. I. Franquesa,  
55 K. Beyer and F. E. Borràs, *Sci. Rep.*, 2016, **6**, 33641.  
56  
57  
58  
59  
60

- 1
  - 2
  - 3
  - 4
  - 5
  - 6
  - 7
  - 8
  - 9
  - 10
  - 11
  - 12
  - 13
  - 14
  - 15
  - 16
  - 17
  - 18
  - 19
  - 20
  - 21
  - 22
  - 23
  - 24
  - 25
  - 26
  - 27
  - 28
  - 29
  - 30
  - 31
  - 32
  - 33
  - 34
  - 35
  - 36
  - 37
  - 38
  - 39
  - 40
  - 41
  - 42
  - 43
  - 44
  - 45
  - 46
  - 47
  - 48
  - 49
  - 50
  - 51
  - 52
  - 53
  - 54
  - 55
  - 56
  - 57
  - 58
  - 59
  - 60
51. H. Zhang, D. Freitas, H. S. Kim, K. Fabijanic, Z. Li, H. Chen, M. T. Mark, H. Molina, A. B. Martin, L. Bojmar, J. Fang, S. Rampersaud, A. Hoshino, I. Matei, C. M. Kenific, M. Nakajima, A. P. Mutvei, P. Sansone, W. Buehring, H. Wang, J. P. Jimenez, L. Cohen-Gould, N. Paknejad, M. Brendel, K. Manova-Todorova, A. Magalhães, J. A. Ferreira, H. Osório, A. M. Silva, A. Massey, J. R. Cubillos-Ruiz, G. Galletti, P. Giannakakou, A. M. Cuervo, J. Blenis, R. Schwartz, M. S. Brady, H. Peinado, J. Bromberg, H. Matsui, C. A. Reis and D. Lyden, *Nat. Cell Biol.*, 2018, **20**, 332-343.
52. R. Stranska, L. Gysbrechts, J. Wouters, P. Vermeersch, K. Bloch, D. Dierickx, G. Andrei and R. Snoeck, *J. Transl. Med.*, 2018, **16**, 1.
53. M. Macías, V. Rebmann, B. Mateos, N. Varo, J. L. Perez-Gracia, E. Alegre and Á. González, *Clin. Chem. Lab. Med.*, 2019, **57**, 1539-1545.
54. T. F. Bruce, T. J. Slonecki, L. Wang, S. Huang, R. R. Powell and R. K. Marcus, *Electrophoresis*, 2019, **40**, 571-581.
55. L. Wang, T. F. Bruce, S. Huang and R. K. Marcus, *Anal. Chim. Acta*, 2019, **1082**, 186-193.
56. S. Huang, L. Wang, T. F. Bruce and R. K. Marcus, *Anal. Bioanal. Chem.*, 2019, **411**, 6591-6601.
57. K. K. Jackson, R. R. Powell, T. F. Bruce and R. K. Marcus, *Anal. Bioanal. Chem.*, 2020, **412**, 4713-4724.
58. S. Huang, L. Wang, T. F. Bruce and R. K. Marcus, *Biotechnol. Prog.*, 2020, e2998.
59. X. Ji, S. Huang, J. Zhang, T. F. Bruce, Z. Tan, D. Wang, J. Zhu, R. K. Marcus and D. M. Lubman, *Electrophoresis*, 2021, **42**, 245-256.
60. S. Huang, X. Ji, K. K. Jackson, T. F. Bruce, D. M. Lubman and R. K. Marcus, *Anal. Chim. Acta*, 2021, **in press**.
61. L. Wang and R. K. Marcus, *J. Chromatogr. A*, 2019, **1585**, 161-171.
62. J. Fausnaugh and F. Regnier, *J. Chromatogr. A*, 1986, **359**, 131-146.
63. A. Jungbauer, C. Machold and R. Hahn, *J. Chromatogr. A*, 2005, **1079**, 221-228.
64. J. A. Queiroz, C. T. Tomaz and J. M. Cabral, *J. Biotechnol.*, 2001, **87**, 143-159.
65. S. Sitar, A. Kežar, D. Pahovnik, K. Kogej, M. Tušek-Žnidarič, M. Lenassi and E. Žagar, *Anal. Chem.*, 2015, **87**, 9225-9233.
66. B. Vestad, A. Llorente, A. Neurauder, S. Phuyal, B. Kierulf, P. Kierulf, T. Skotland, K. Sandvig, K. B. F. Haug and R. Øvstebø, *J. Extracell. Vesicles*, 2017, **6**, 1344087.
67. Z. Andreu and M. Yanez-Mo, *Front. Immunol.*, 2014, **5**, 442.
68. E. Willms, C. Cabanas, I. Mager, M. J. A. Wood and P. Vader, *Front. Immunol.*, 2018, **9**, 738.
69. V. Vagenende, A. X. Han, M. Mueller and B. L. Trout, *Chem. Biol.*, 2013, **8**, 416-422.
70. V. Vagenende, M. G. Yap and B. L. Trout, *Biochem.*, 2009, **48**, 11084-11096.
71. B. E. Saxberg and B. R. Kowalski, *Anal. Chem.*, 1979, **51**, 1031-1038.
72. K. Vaswani, M. D. Mitchell, O. J. Holland, Y. Qin Koh, R. J. Hill, T. Harb, P. S. W. Davies and H. Peiris, *J. Nutr. Metabol.*, 2019, **2019**, 5764740.
73. L. Musante, S. V. Bontha, S. La Salvia, A. Fernandez-Piñeros, J. Lannigan, T. H. Le, V. Mas and U. Erdbrügger, *Sci. Rep.*, 2020, **10**, 3701.

- 1  
2  
3 74. S. R. Kumar, E. T. Kimchi, Y. Manjunath, S. Gajagowni, A. J. Stuckel and J. T.  
4 Kaifi, *Sci. Rep.*, 2020, **10**, 2800.  
5 75. P. J. Wermuth, S. Piera-Velazquez and S. A. Jimenez, *Clin. Exp. Rheumatol.*,  
6 2017, **35 Suppl 106**, 21-30.  
7 76. C. Conzelmann, R. Groß, M. Zou, F. Krüger, A. Görgens, M. O. Gustafsson, S.  
8 El Andaloussi, J. Münch and J. A. Müller, *J. Extracell. Vesicles*, 2020, **9**,  
9 1808281.  
10  
11  
12  
13  
14  
15  
16  
17  
18  
19  
20  
21  
22  
23  
24  
25  
26  
27  
28  
29  
30  
31  
32  
33  
34  
35  
36  
37  
38  
39  
40  
41  
42  
43  
44  
45  
46  
47  
48  
49  
50  
51  
52  
53  
54  
55  
56  
57  
58  
59  
60

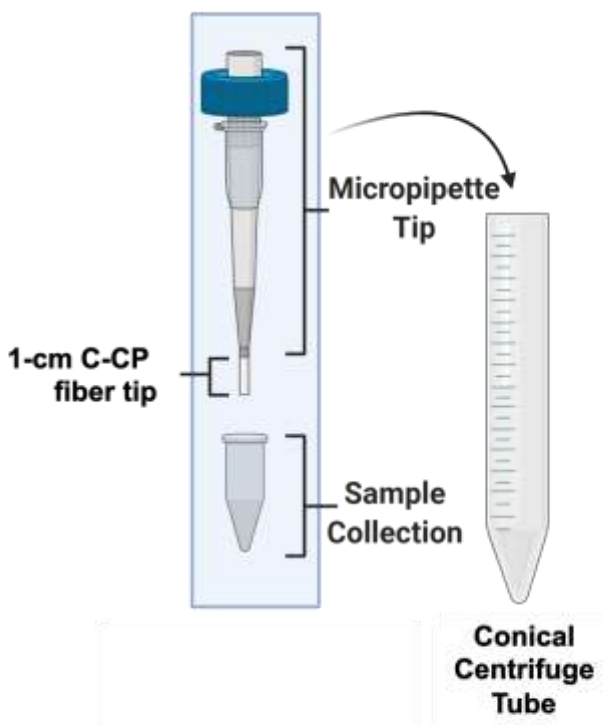


Figure 1

Figure 1: The capillary-channeled polymer (C-CP) fiber solid-phase extraction tip setup for the isolation of EVs from complex biofluids in a tabletop centrifuge.

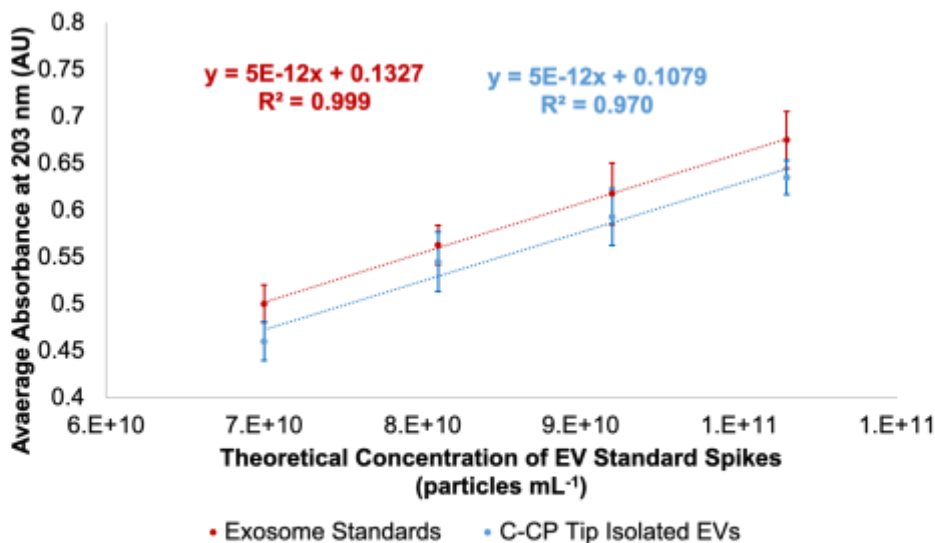


Figure 2

Figure 2: Standard addition curve using a commercial exosome standard stock of  $1.1 \times 10^{10}$  particles per mL concentration based on absorbance measurement at 203 nm (red). Quantification of EVs based on absorbance detection after employing aqueous EV solutions of known concentration to the C-CP tip (blue).

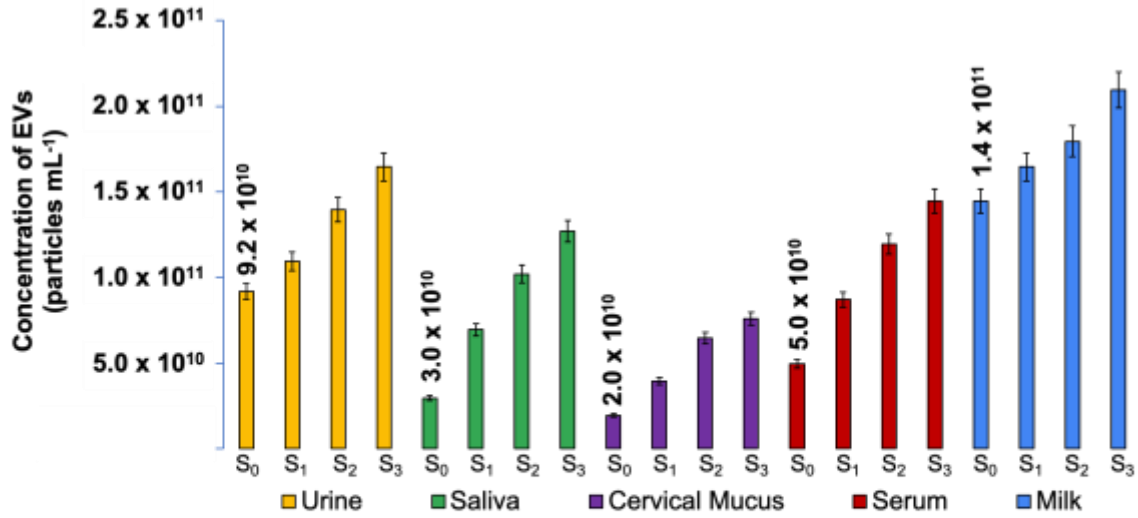


Figure 3

Figure 3: Determined EV particle concentrations ( $n=3$ ) for human urine, saliva, cervical mucus, blood serum and goat milk biofluid unknown samples spiked once, twice, and three times with a commercial exosome standard stock of  $1.1 \times 10^{10}$  particle per mL before EV isolation using the C-CP tip workflow. The biofluid-originating EV recoveries were quantified based on absorbance at 203 nm and compared to a response curve of linear response.

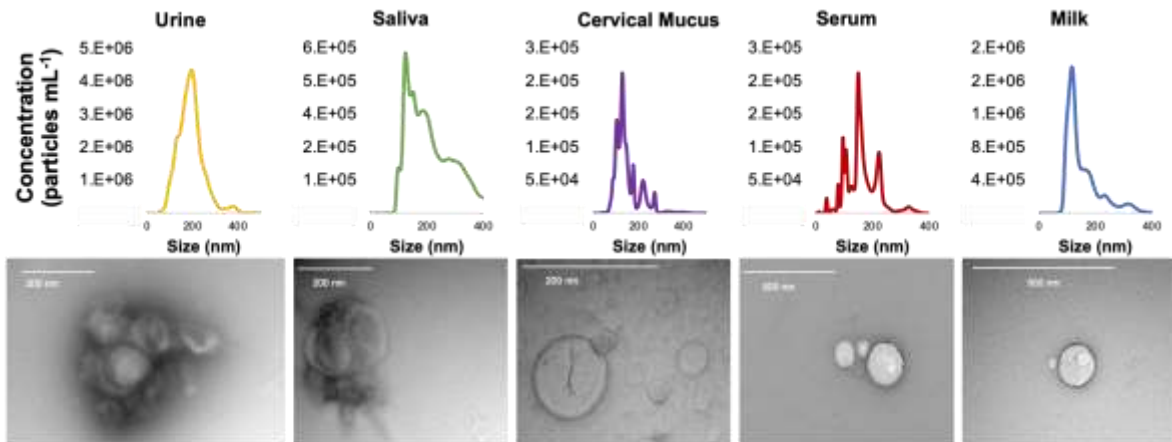


Figure 4

Figure 4: Size distribution of vesicles in the EV recoveries resulting from the C-CP fiber tip isolation from human urine, saliva, cervical mucus, blood serum, and goat milk, measured using the Nanosight NS300 nanoparticle tracking analysis system. TEM micrographs of EVs isolated from biofluids using the C-CP fiber tip, taken using the Hitachi HT7830.



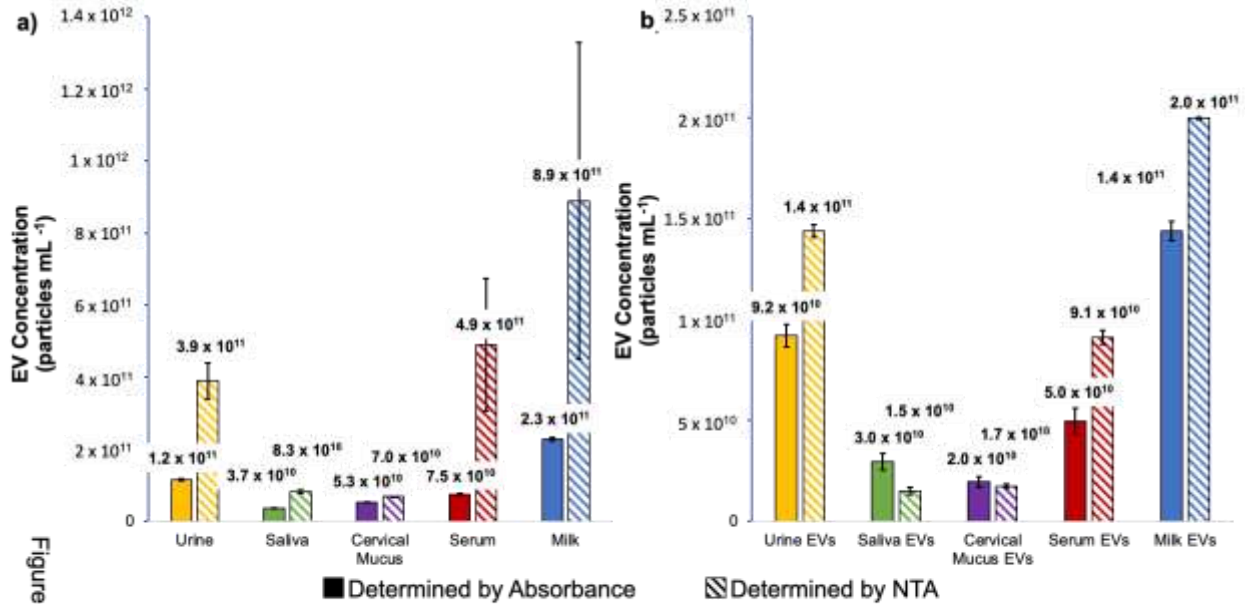


Figure 5

Figure 5: Comparison of the determined concentration of a) EVs in each bulk biofluid sample and b) EVs recovered from each biofluid using the C-CP tip method as determined using the method of standard addition by absorbance at 203 nm and by nanoparticle tracking analysis.

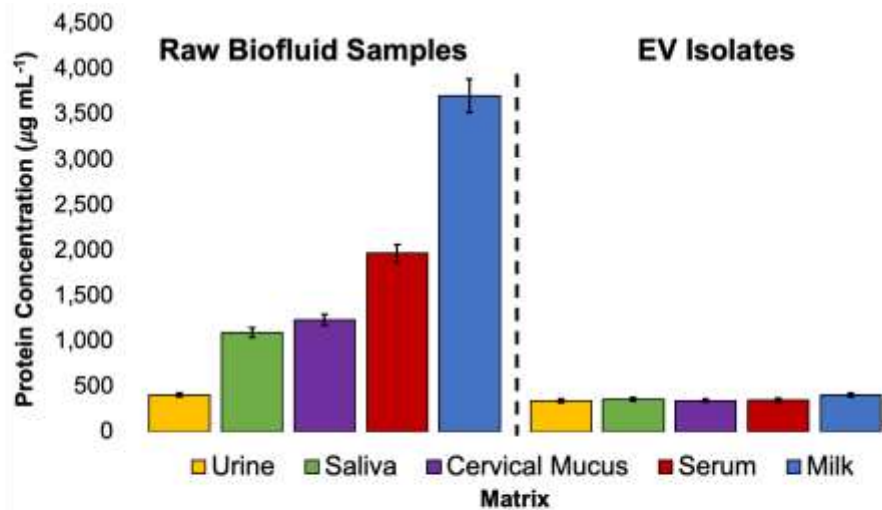


Figure 6

Figure 6: Bradford assay of raw biofluid matrices and concentrated EV recoveries after isolation with the C-CP tip. The total protein concentration was determined using the absorbance measurement of Bradford reagent at 595 nm, as compared to a BSA standard curve of linear response. n = 3

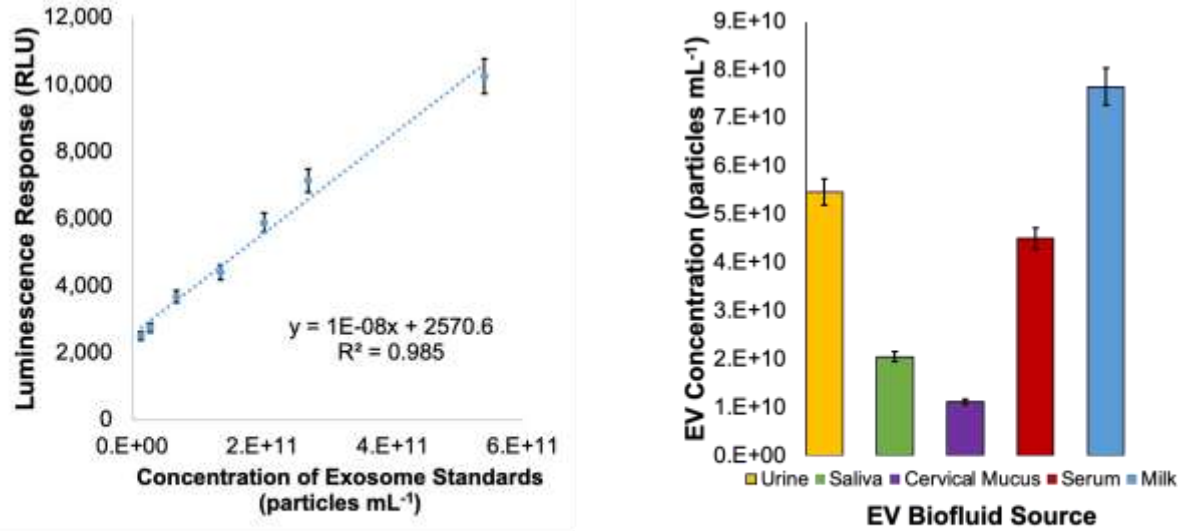


Figure 7 *Indirect ELISA standard curve employing an antibody to the CD81 tetraspanin protein using serial dilutions of a commercial exosome standard ( $2.7 \times 10^{12}$  particles per mL), and the CD81 responses of the C-CP tip isolated EVs from biofluid samples.*